FULL PAPER

Dalton
www.rsc.org/dalton

Single-molecule magnets. A Mn_{12} complex with mixed carboxylate-sulfonate ligation: $[Mn_{12}O_{12}(O_2CMe)_8(O_3SPh)_8(H_2O)_4]$

Nicole E. Chakov,[a] Wolfgang Wernsdorfer,[b] Khalil A. Abboud,[a] David N. Hendrickson[c] and George Christou*[a]

[a] *Department of Chemistry, University of Florida, Gainesville, FL 32611-7200, USA. E-mail: christou@chem.ufl.edu*

[b] *Laboratoire Louis Néel-CNRS, BP166, 25 Avenue des Martyrs, 38042 Grenoble, Cedex 9, France*

[c] *Department of Chemistry–0358, University of California at San Diego, La Jolla, CA 92093-0358, USA*

Received 14th February 2003, Accepted 3rd April 2003
First published as an Advance Article on the web 17th April 2003

The synthesis and magnetic properties of a new member of the Mn_{12} single-molecule magnet family, $[Mn_{12}O_{12}(O_2CMe)_8(O_3SPh)_8(H_2O)_4]$ (**2**), are reported. The compound was prepared by treatment of $[Mn_{12}O_{12}(O_2CMe)_{16}(H_2O)_4]$ (**1**) with eight equivalents of $PhSO_3H$ in MeCN. Complex **2**·$4CH_2Cl_2$ crystallizes in the triclinic space group $P\bar{1}$. The complex consists of a central $[Mn^{IV}_4O_4]$ cubane held within a nonplanar ring of eight Mn^{III} ions by eight μ_3-O^{2-} ions. Eight bridging acetate groups occupying equatorial sites, eight bridging benzenesulfonate groups in axial sites, and four terminal water molecules complete the peripheral ligation of the molecule. The spin of the ground state was established by magnetization measurements in the 2.00–7.00 T field range and 1.80–4.00 K temperature range. Fitting of the reduced magnetization data by full matrix diagonalization, incorporating only axial anisotropy, gave $S = 10$, $g = 1.96$ and $D = -0.34$ cm^{-1}. The cluster exhibits out-of-phase ac susceptibility signals and temperature-dependent hysteresis loops at temperatures below 4.00 K, establishing **2** as a new single-molecule magnet.

Introduction

One of the primary reasons for the current interest in high nuclearity Mn carboxylate clusters is the study of single-molecule magnets (SMMs). A SMM possesses a significant energy barrier to relaxation (reorientation) of its magnetization vector, owing to a combination of a large ground state spin (S) value and a large easy-axis type of magnetoanisotropy (negative axial zero-field splitting parameter, D). The upper limit of the energy barrier is given by $S^2|D|$ or $(S^2 - ¼)|D|$ for integer and non-integer spins, respectively.[1,2] The SMMs with the largest energy barriers to date are the $[Mn_{12}O_{12}(O_2CR)_{16}(H_2O)_4]$ (Mn_{12}) family, and they have thus received a great deal of attention.

Amongst the many studies that we have performed on Mn_{12} complexes have been attempts to derivatize them with non-carboxylate ligands in a site-specific manner, in order to direct or enhance reactivity at selected sites and thus make regioselective reactions feasible. Such selectivity would be important for achieving clean and controllable reactivity in a complex containing so many carboxylate groups, and would make more feasible important objectives such as the binding of groups that might enhance the shape anisotropy or magnetic properties of the Mn_{12} complexes, and/or facilitate the binding of the latter to surfaces, or to each other to give dimers (or higher aggregates) of Mn_{12} species. One objective has been to replace just the eight axial, or just the eight equatorial carboxylate groups with non-carboxylate ones, and thus obtain a mixed-ligand derivative with the two types of groups in specific positions on the Mn_{12} molecule. Unfortunately, our previous attempts have met with limited success, and we have been unable to substitute all axial or all equatorial carboxylate ligands with non-carboxylate groups to date. For example, four (but no more) of the eight axial carboxylate groups could be replaced with NO_3^- groups using nitric acid, giving $[Mn_{12}O_{12}(NO_3)_4(O_2CCH_2Bu^t)_{12}(H_2O)_4]$;[3] additional equivalents of nitric acid caused decomposition. This incorporation of nitrate was a useful step forward but did not fulfill our desire to functionalize all axial sites with non-carboxylate ligands. Similarly, we have been able to replace eight of the carboxylate groups with diphenylphosphinates ($Ph_2PO_2^-$) to give $[Mn_{12}O_{12}(O_2PPh_2)_8(O_2CCH_3)_8(H_2O)_4]$,[4] but the steric bulk of the $Ph_2PO_2^-$ groups resulted in them distributing themselves equally between axial and equatorial sites.

However, we can now report achievement of the above goal by the introduction into all the axial sites of benzenesulfonate groups, $PhSO_3^-$, with retention of the Mn_{12} structure and its SMM properties. This also represents the first incorporation of S-based ligands into the Mn_{12} SMMs. The synthesis, structure, and magnetic properties of the obtained complex are described.

Experimental

Synthesis

All manipulations were performed under aerobic conditions using chemicals as received, unless otherwise stated. $[Mn_{12}O_{12}(O_2CMe)_{16}(H_2O)_4]$ (**1**) was prepared as described in the literature.[5]

$[Mn_{12}O_{12}(O_2CMe)_8(O_3SPh)_8(H_2O)_4]$ (2). A solution of complex **1** (1.00 g, 0.54 mmol) in MeCN was treated with $PhSO_3H$ (0.68 g, 4.30 mmol) in MeCN (25 mL). The solution was stirred overnight and the solvent was removed. Toluene (25 mL) was added to the residue, and the solution was evaporated to dryness. The addition and removal of toluene was repeated three more times. The residue was dissolved in CH_2Cl_2 (50 mL) and filtered. An equal volume of hexanes was added to the filtrate, and the solution was allowed to stand at room temperature for 4 days. Black crystals of **2**·$4CH_2Cl_2$ were collected by filtration, washed with hexanes, and dried *in vacuo*. The yield was 1.37 g (96%). Calc. (Found) for **2**·$3CH_2Cl_2$ ($C_{67}H_{78}Mn_{12}O_{56}S_8Cl_6$): C, 27.67 (27.81); H, 2.70 (2.80); N, 0.00 (0.07)%. Selected IR data (cm^{-1}): 1506(s); 1446(vs); 1245(m); 1203(m); 1127(s); 1037(m); 1018(s); 996(m); 981(m); 757(w); 732(m); 690(s); 671(s); 607(vs); 564(s).

$[Mn_{12}O_{12}(O_2CMe)_{12}(O_3SPh)_4(H_2O)_4]$ (3). A solution of complex **1** (0.50 g, 0.27 mmol) in MeCN was treated with $PhSO_3H$ (0.17 g, 1.07 mmol) in MeCN (25 mL). The solution was stirred

DOI: 10.1039/b301785k

overnight, and the solvent was then removed. Toluene (25 mL) was added to the residue, and the solution was evaporated to dryness. The addition and removal of toluene was repeated three more times. The residue was dissolved in CH_2Cl_2 (25 mL) and filtered. An equal volume of hexanes was added to the filtrate, and the solution allowed to stand at room temperature for ~4 days. Black crystals of **3** were collected by filtration, washed with hexanes, and dried *in vacuo*. The yield was 0.49 g (81%). Calc. (Found) for **3** ($C_{48}H_{64}Mn_{12}O_{52}S_4$): C, 25.50 (25.73); H, 2.85 (3.24); N, 0.00 (0.02)%. Selected IR data (cm^{-1}): 1576(m); 1506(m); 1447(vs); 1330(m); 1192(s); 1128(s); 1039(m); 1019(s); 997(m); 761(w); 731(m); 673(vs); 646(s); 607(vs).

X-Ray crystallography and solution of structure

Data were collected using a Siemens SMART PLATFORM equipped with a CCD area detector and a graphite monochromator utilizing Mo-Kα radiation (λ = 0.71073 Å). A suitable crystal of **2**·4CH_2Cl_2 was attached to a glass fibre using silicone grease and transferred to the goniostat where it was cooled to 193 K for characterization and data collection. A preliminary search of reciprocal space revealed a triclinic unit cell; the choice of the space group $P\bar{1}$ was confirmed by the subsequent solution and refinement of the structure. Cell parameters were refined using up to 8192 reflections. A full sphere of data (1381 frames) was collected using the ω-scan method (0.3° frame width). The first 50 frames were re-measured at the end of data collection to monitor instrument and crystal stability (maximum correction on I was <1 %). Absorption corrections by integration were applied based on measured indexed crystal faces.

The structure was solved using a combination of direct methods (SHELXTL5)[6] and Fourier techniques. The asymmetric unit consists of the Mn_{12} cluster and four CH_2Cl_2 molecules of crystallization. Two of the CH_2Cl_2 molecules are disordered. In one of them, the Cl atoms were disordered over three positions and their site occupation factors refined to 0.85(1), 0.17(1) and 0.08(1). The second disordered molecule has its Cl atoms in two sets of sites with site occupation factors refined to 0.56(1) and 0.44(1). The non-H atoms were treated anisotropically. All hydrogen atoms (except for those on the water groups) were calculated in idealized positions on their respective carbon atoms. The water H atoms were not found in any difference Fourier map. A total of 1406 parameters were refined in the final cycle of refinement using 16674 reflections with $I > 2\sigma(I)$ to yield R_1 and wR_2 of 3.79% and 9.90%, respectively. Refinement was done using F^2. Table 1 lists the unit cell and structure refinement data for **2**·4CH_2Cl_2.

CCDC reference number 191072.

See http://www.rsc.org/suppdata/dt/b3/b301785k/ for crystallographic data in CIF or other electronic format.

Other measurements

Infrared spectra were recorded in the solid state (KBr pellets) on a Nicolet Nexus 670 FTIR spectrophotometer in the 4000–400 cm^{-1} range. Elemental analyses (C, H and N) were performed at the in-house facilities of the University of Florida Chemistry Department. Variable-temperature dc magnetic susceptibility data down to 1.80 K were collected on a Quantum Design MPMS-XL SQUID magnetometer equipped with a 7 Tesla dc magnet at the University of Florida. Pascal's constants were used to estimate the diamagnetic corrections, which were subtracted from the experimental susceptibility to give the molar magnetic susceptibility (χ_M). Ac magnetic susceptibility data were collected on the same instrument employing a 0.35 mT field oscillating at frequencies up to 1500 Hz. Dc measurements below 1.80 K were performed on single crystals using an array of micro-SQUIDS.[7]

Table 1 Crystallographic data for $[Mn_{12}O_{12}(O_2CMe)_8(O_3SPh)_8(H_2O)_4]$·4$CH_2Cl_2$ (**2**·4CH_2Cl_2)

Formula[a]	$C_{68}H_{80}Cl_8Mn_{12}O_{56}S_8$
M	2992.76
Space group	$P\bar{1}$
a/Å	15.9971(6)
b/Å	16.0923(7)
c/Å	22.0964(9)
α/°	94.742(2)
β/°	90.307(2)
γ/°	104.262(2)
V/Å^3	5492.1(4)
Z	2
D_c/g cm^{-3}	1.810
T/°C	−80
λ(Mo-Kα)/Å[b]	0.71073
μ(Mo-Kα)/cm^{-1}	17.69
R (R_w)[c](%)	3.79 (9.90)

[a] Including solvate molecules. [b] Graphite monochromator. [c] $R = \Sigma||F_o| - |F_c||/\Sigma|F_o|$; $R_w = [\Sigma[w(F_o^2 - F_c^2)^2]/\Sigma[w(F_o^2)^2]]^{1/2}$, where $w = 1/[\sigma^2(F_o^2) + (0.0565p)^2 + 0.00p]$ and $p = [\max(F_o^2,0) + 2F_c^2]/3$.

Results and discussion

Synthesis

Our previous development and use of ligand substitution reactions on readily available complex **1** have allowed us access to $[Mn_{12}O_{12}(O_2CR)_{16}(H_2O)_4]$ derivatives with a large variety of R groups. The ligand substitution reaction (eqn. (1)) is an equilibrium that must be driven to completion by (i) using a carboxylic acid with a much lower pK_a than that of acetic acid (4.76); and/or (ii) using an excess of RCO_2H; and/or (iii) removing the acetic acid as its toluene azeotrope.

$$[Mn_{12}O_{12}(O_2CMe)_{16}(H_2O)_4] + 16\,RCO_2H \rightleftharpoons [Mn_{12}O_{12}(O_2CR)_{16}(H_2O)_4] + 16\,MeCO_2H \quad (1)$$

The latter is particularly useful for incorporating carboxylate groups whose conjugate acid has a pK_a comparable to, or even higher than that of acetic acid. The substitution reaction has been successfully employed for ligands such as benzoate (and substituted benzoates), and a variety of alkanecarboxylates.[8] Of relevance to the present work is the fact that the substitution procedure has already been extended to non-carboxylate ligands in the successful incorporation of $Ph_2PO_2^-$ groups,[4] as mentioned above. Thus, the reactions of **1** with another type of organic acid were explored, namely benzenesulfonic acid (pK_a = 2.55).

The reaction of complex **1** with eight equivalents of benzenesulfonic acid ($PhSO_3H$) in MeCN was followed by several cycles of addition of toluene and its removal under vacuum. Note that since only partial replacement of acetate groups was being sought, excess acid could not be added, and the removal of acetic acid as the toluene azeotrope thus was an essential step to ensure complete reaction. This procedure successfully led to the isolation and crystallization of $[Mn_{12}O_{12}(O_2CMe)_8(O_3SPh)_8(H_2O)_4]$ (**2**) in essentially quantitative (96%) yield (eqn. (2)).

$$[Mn_{12}O_{12}(O_2CMe)_{16}(H_2O)_4] + 8\,PhSO_3H \longrightarrow [Mn_{12}O_{12}(O_2CMe)_8(O_3SPh)_8(H_2O)_4] + 8\,MeCO_2H \quad (2)$$

Crystallization from CH_2Cl_2–hexanes gave dark brown crystals of **2**·4CH_2Cl_2 suitable for X-ray crystallography.

Similarly, the reaction of **1** with four equivalents of $PhSO_3H$ leads to the formation of $[Mn_{12}O_{12}(O_2CMe)_{12}(O_3SPh)_4(H_2O)_4]$, whose identity was established by elemental analysis and spectroscopic comparison with **2**. This is summarized in eqn. (3).

$$[Mn_{12}O_{12}(O_2CMe)_{16}(H_2O)_4] + 4\,PhSO_3H \longrightarrow [Mn_{12}O_{12}(O_2CMe)_{12}(O_3SPh)_4(H_2O)_4] + 4\,MeCO_2H \quad (3)$$

Reactions of $PhSO_3H$ with other Mn carboxylate complexes, including $[Mn_3O(O_2CR)_6(py)_3]^{0,+}$ and $[Mn_4O_2(O_2CPh)_9(H_2O)]^-$, have also been carried out, but attempts to crystallographically characterize the products have all been unsuccessful to date.

The carboxylate substitution with benzenesulfonate is reversible on treatment of **2** with eight equivalents of $MeCO_2H$ in CH_2Cl_2, supporting the feasibility of using **2** for reactions directed at site-specific replacement of axial $PhSO_3^-$ ligands by some added reagent, taking advantage of the good leaving properties of this group.

Crystal structure

A labeled ORTEP[9] plot of complex **2** is presented in Fig. 1, and selected bond distances and angles are listed in Table 2.

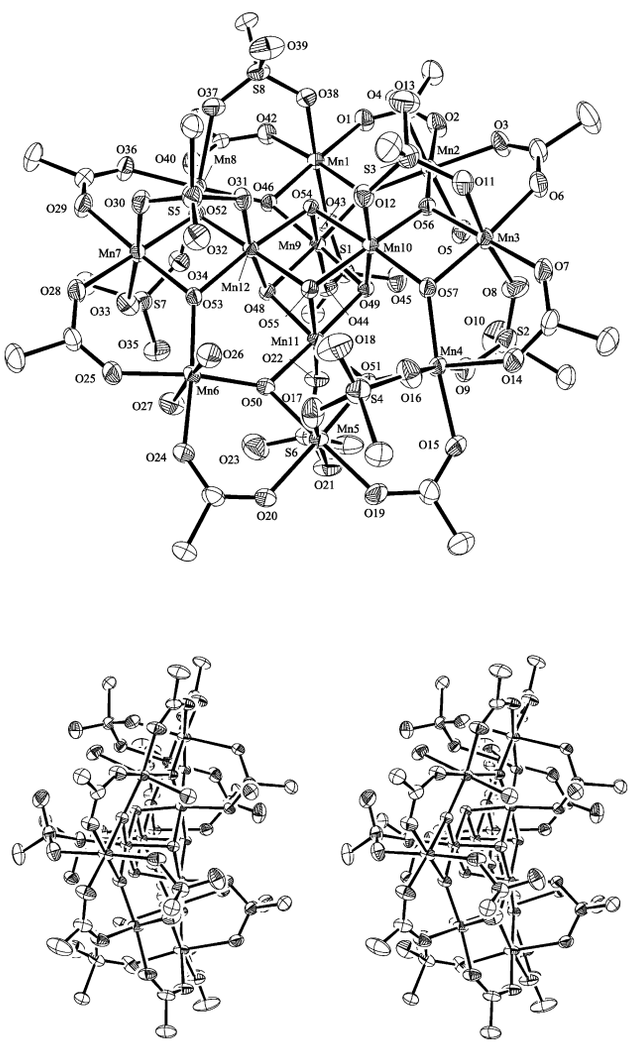

Fig. 1 ORTEP representation and stereoview of $[Mn_{12}O_{12}(O_2CMe)_8(O_3SPh)_8(H_2O)_4]$ (**2**) with the atoms drawn at the 50% probability level. Hydrogen atoms have been omitted for clarity. Only the *ipso* carbon atoms of the phenyl groups are shown.

Complex **2**·$4CH_2Cl_2$ crystallizes in the triclinic space group $P\bar{1}$ with the asymmetric unit consisting of one Mn_{12} molecule and four CH_2Cl_2 molecules of crystallization. The Mn_{12} cluster possesses an overall structure similar to that of complex **1**, with a central $[Mn^{IV}_4O_4]$ cubane held within a non-planar ring of eight Mn^{III} ions by eight μ_3-O^{2-} ions. The eight Mn^{III} ions separate into two groups of four Mn^{III} ions each. In the first group, each Mn^{III} ion is coordinated to a single Mn^{IV} ion *via* two oxide bridges (Mn1, Mn3, Mn5, Mn7), while in the second group each Mn^{III} ion is coordinated to two Mn^{IV} ions *via* two oxide bridges (Mn2, Mn4, Mn6, Mn8).[10] Four water molecules, eight

Table 2 Selected interatomic distances (Å) and angles (°) for $[Mn_{12}O_{12}(O_2CMe)_8(O_3SPh)_8(H_2O)_4]$ (**2**)

Mn^{IV}–O_c (ax)[a]	1.863(2)–1.876(2)
Mn^{IV}–O_c (eq)	1.9157(19)–1.9393(19)
Mn^{IV}–O_r	1.854(2)–1.874(2)
Mn^{IV}–O_{ax}	1.907(2)–1.945(2)
Mn^{IIIb}–O_r[b]	1.883(2)–1.909(2)
Mn^{IIIc}–O_r[c]	1.880(2)–1.910(2)
Mn^{IIIb}–O_{eq}	1.920(2)–1.942(2)
Mn^{IIIc}–O_{eq}	1.929(2)–1.963(2)
Mn^{IIIb}–O_{ax}	2.163(2)–2.262(2)
Mn^{IIIc}–O_{ax}	2.174(2)–2.190(2)
Mn^{IIIc}–O_w	2.216(2)–2.222(2)
O_r–Mn^{IV}–O_r	83.27(9)–84.13(9)
O_r–Mn^{IIIb}–O_r	81.70(9)–82.74(8)
O_r–Mn^{IIIc}–O_r	94.83(8)–95.52(9)
$Mn^{IV} \cdots Mn^{IV}$	2.8054(6)–2.9478(6)
$Mn^{IIIb} \cdots Mn^{IIIc}$	3.352–3.454
$Mn^{IIIb} \cdots Mn^{IV} \cdots Mn^{IV}$	175.99(2)–178.21(2)
$Mn^{IIIb} \cdots Mn^{IV}$	2.7905(6)–2.8016(6)
$Mn^{IIIc} \cdots Mn^{IV}$	3.416–3.466

[a] O_c = cubane O^{2-}, O_r = ring O^{2-}, O_{ax} = axial carboxylate, O_{eq} = equatorial carboxylate, O_w = water. [b] Mn^{IIIb} atoms: Mn(1,3,5,7); [c] Mn^{IIIc} atoms: Mn(2,4,6,8).

μ-carboxylate and eight μ-benzenesulfonate groups complete the peripheral ligation about the $[Mn_{12}O_{12}]$ core of the complex. The eight Mn^{III} centers exhibit a Jahn–Teller (JT) distortion, as expected for a high-spin d^4 ion in near octahedral geometry. As is almost always the case for Mn^{III}, the JT distortion in **2** takes the form of an axial elongation of two *trans* bonds. Again as is usually the case, the JT elongation axes avoid the Mn–O^{2-} bonds, the shortest and strongest in the molecule, and thus the JT axes are all axially disposed, roughly perpendicular to the $[Mn_{12}O_{12}]$ disk-like core. As a result, there is a near parallel alignment of the eight Mn^{III} JT elongation axes. This is also the origin of the significant magnetic anisotropy in the *z* direction that greatly influences the observed magnetic properties (*vide infra*).

The $MeCO_2^-$ groups occupy the eight equatorial sites of **2**, while the $PhSO_3^-$ ligands are located at the eight axial sites above and below the disk-like $[Mn_{12}O_{12}]$ core. This selectivity in axial *vs*. equatorial binding sites can be rationalized on the basis of the relative basicities of acetate *vs*. benzenesulfonate. The pK_a value of $PhSO_3H$ is 2.55 while that of $MeCO_2H$ is 4.76. The more basic, stronger donor $MeCO_2^-$ ligands favor occupation of the equatorial sites where shorter, stronger Mn–O bonds can be formed, to the benefit of the overall energy stabilization of the molecule.[11] The less basic $PhSO_3^-$ ligands thus occupy axial positions where they bridge either $Mn^{III}Mn^{III}$ or $Mn^{III}Mn^{IV}$ pairs and thus have one or both of their O atoms on the JT elongation axes. There are twenty axial coordination sites, of which sixteen lie on JT elongation axes, and these bonds are lengthened by 0.1–0.2 Å and thus are weakened relative to the equatorial, non JT-elongated Mn–carboxylate bonds. The same rationalization based on relative acid pK_a values also explained the selective axial *vs*. equatorial disposition in mixed-carboxylate $[Mn_{12}O_{12}(O_2CR)_8(O_2CR')_8(H_2O)_4]$ complexes.[11]

In all $[Mn_{12}O_{12}(O_2CR)_{16}(H_2O)_4]$ complexes studied to date, the four water ligands coordinate only to the four Mn^{III} ions in the second group described above (Mn2, Mn4, Mn6, Mn8),[12] either one water on each Mn, two each on two Mn, or similar. Indeed, complex **2** similarly has two water ligands, O4 and O5, on a Mn^{III} ion of the second group (Mn2), and two water ligands, O26 and O27, on another Mn^{III} ion of the same group (Mn6). This *trans* disposition of two pairs of H_2O ligands has also been observed for $[Mn_{12}O_{12}(O_2CPh)_{16}(H_2O)_4]$, $[Mn_{12}O_{12}(O_2CC_6H_4Cl\text{-}4)_{16}(H_2O)_4]$ and others.[10,12]

The formation of complex **3** from **1** represents an abstraction of only four carboxylate groups from a $[Mn_{12}O_{12}(O_2CR)_{16}(H_2O)_4]$ complex. This has been previously achieved exclusively

at the axial ligands bridging the $Mn^{III}Mn^{III}$ pairs, where the four bridging carboxylates are the only ones to have *both* their O atoms on JT elongation sites and thus are the most susceptible to substitution. Both $[Mn_{12}O_{12}(NO_3)_4(O_2CR)_{12}(H_2O)_4]$[3] and, subsequently, $[Mn_{12}O_{12}(O_2P(OPh)_2)_4(O_2CPh)_{12}(H_2O)_4]$[13] have been crystallographically confirmed to have their non-carboxylate bridging groups at these positions. Thus, although we have not sought the crystal structure of complex **3**, it is very likely that it has the four $PhSO_3^-$ groups in axial positions bridging the same $Mn^{III}Mn^{III}$ pairs as the NO_3^- and $(PhO)_2PO_2^-$ derivatives.

Magnetochemistry

Dc magnetic susceptibility. Solid-state, variable temperature magnetic susceptibility measurements were performed on a vacuum-dried, powdered sample of complex **2**, suspended in eicosane to prevent torquing. Dc magnetic susceptibility (χ_M) data were collected in the 2.00–300 K range in a 0.5 T magnetic field. The $\chi_M T$ *vs.* T behaviour is similar to those of previously studied $[Mn_{12}O_{12}(O_2CR)_{16}(H_2O)_4]$ complexes with $S = 10$ ground states, exhibiting a nearly temperature-independent $\chi_M T$ value of 21–22 cm^3 K mol^{-1} in the 150–300 K range which then increases rapidly to a maximum value of 45–46 cm^3 K mol^{-1} at ~20 K before decreasing rapidly at lower temperatures. The maximum indicates a large ground state spin (S) value, and the low temperature decrease is primarily due to Zeeman and zero-field splitting (ZFS) effects.

A theoretical treatment of the susceptibility data *via* the Kambé method[14] to determine the individual pairwise Mn_2 exchange interactions was not possible owing to the topological complexity and low symmetry of the Mn_{12} core. Instead, the ground state spin of complex **2** was determined from magnetization (M) measurements in the 1.80–4.00 K temperature range and 2.0–7.0 T field range, where N is Avogadro's number, μ_B is the Bohr magneton, and H is the applied magnetic field. The obtained data are plotted as $(M/N\mu_B)$ *vs.* H/T in Fig. 2. For a system occupying only the ground state and experiencing no ZFS, the various isofield lines would be superimposed and $M/N\mu_B$ would saturate at a value of gS. The non-superposition of the isofield lines in Fig. 2 is indicative of the presence of strong ZFS. The data were fit using the method described elsewhere[15] that involves diagonalization of the spin Hamiltonian matrix, assuming only the ground state is occupied at these temperatures and including axial ZFS ($D\hat{S}_z^2$), Zeeman interactions, and a full powder average of the magnetization. The obtained fit of the data, shown as solid lines in Fig. 2, gave $S = 10$, $g = 1.96$ and $D \sim -0.34$ cm^{-1} (−0.49 K).[16] Thus, complex **2** retains the same spin as **1**, with fitting parameters typical for $[Mn_{12}O_{12}(O_2CR)_{16}(H_2O)_4]$ clusters. The poorer quality of the fit than is typically found for $[Mn_{12}O_{12}(O_2CR)_{16}(H_2O)_4]$ complexes likely results from population of an excited state of the cluster that is lower-lying than normal; thus, the obtained D value must be considered as only a rough approximation.[11] The $S = 10$ value shows that, as previously seen with the mixed-carboxylate $[Mn_{12}O_{12}(O_2CR)_8(O_2CR')_8(H_2O)_4]$ clusters, the presence of two types of ligands with distinctly different basicities does not affect the large ground state S value of the Mn_{12} complex.[11]

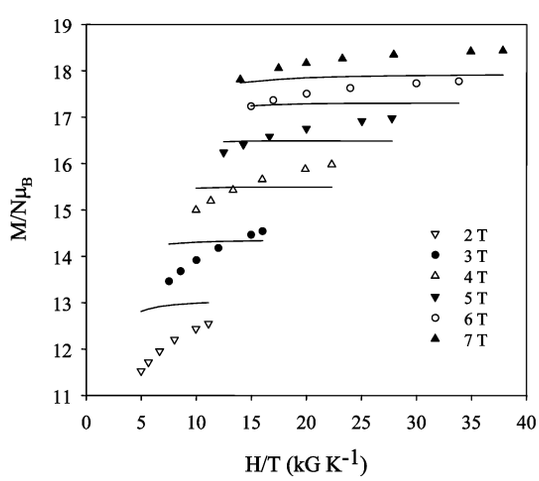

Fig. 2 Plot of reduced magnetization ($M/N\mu_B$) *vs.* H/T for complex **2** in applied fields of 2 (▽), 3 (●), 4 (△), 5 (▼), 6 (○) and 7 (▲) Tesla. The solid lines are the fit of the data; see the text for the fitting parameters.

Ac magnetic susceptibility. In an ac susceptibility experiment, a weak field (typically 0.1–0.5 mT) oscillating at a particular frequency (ν) is applied to a sample to probe the dynamics of the magnetization (magnetic moment) relaxation. An out-of-phase ac susceptibility signal (χ_M'') is observed when the rate at which the magnetization of a molecule relaxes is close to the operating frequency of the ac field, and there is a corresponding decrease in the in-phase ($\chi_M' T$) signal. At low enough temperature, where the thermal energy is lower than the barrier for relaxation, the magnetization of the molecule cannot relax fast enough to keep in-phase with the oscillating field. Therefore, the molecule will exhibit a frequency-dependent χ_M'' signal indicative of slow magnetization relaxation. Frequency-dependent χ_M'' signals are an important indicator of SMMs.

Ac susceptibility studies were performed on complex **2** in the 1.80–10.0 K range in a 0.35 mT field oscillating at frequencies (ν) up to 1000 Hz. The in-phase (χ_M') signal (as $\chi_M' T$) and out-of-phase (χ_M'') signal are plotted *vs.* T in Fig. 3. Clearly evident are a frequency-dependent decrease in $\chi_M' T$ at $T < 10$ K, concomitant with the appearance of a frequency-dependent out-of-phase (χ_M'') signal. These indicate that the magnetization of **2** cannot relax fast enough to stay in-phase with the oscillating field, and this is a strong indication that complex **2** is a single-molecule magnet (SMM). Note that at each frequency there is only one χ_M'' peak, and complex **2** does not therefore exhibit JT isomerism. The latter is the presence of an abnormally oriented

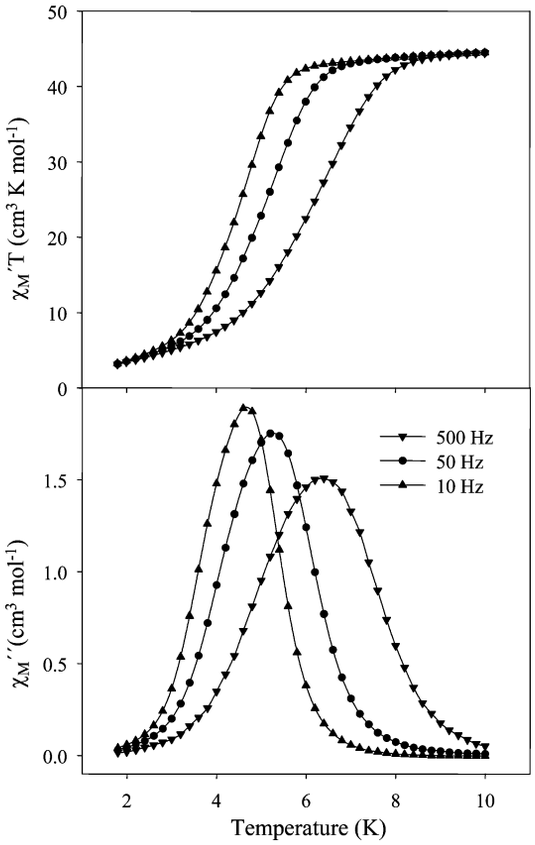

Fig. 3 Plot of the in-phase (as $\chi_M' T$) and out-of-phase (χ_M'') ac susceptibility signals *vs.* temperature for complex **2** at the indicated oscillation frequencies.

JT axis, equatorial with respect to the Mn_{12} disk, that leads to a lower barrier to magnetization relaxation and a χ_M'' peak at consequently lower temperatures.[17,18] Complex **2** is thus present as exclusively the normal, slower-relaxing JT isomer.

Relaxation studies using ac and dc data. The χ_M'' *vs.* T plots were used as a source of kinetic data to calculate the effective energy barrier (U_{eff}) to magnetization relaxation. At a given oscillation frequency (ν), the position of the χ_M'' peak maximum is the temperature at which the angular frequency ($\omega = 2\pi\nu$) of the oscillating field equals the relaxation rate ($1/\tau$, where τ is the relaxation time) at which a molecule's magnetization vector relaxes between one orientation along the easy axis (the z axis) to the opposite one. The relaxation rates at a given temperature can thus be obtained from $\omega = 1/\tau$ at the maxima of the χ_M'' peaks. The peak maxima were accurately determined by fitting the peaks to a Lorentzian function.

The magnetization relaxation of a SMM obeys the Arrhenius relationship (eqn. (4)), the characteristic behavior of a thermally activated Orbach process,[19] where U_{eff} is the effective anisotropy energy barrier and k is the Boltzmann constant.

$$(1/\tau) = (1/\tau_0)\exp(-U_{eff}/kT) \quad (4a)$$

$$\ln(1/\tau) = \ln(1/\tau_0) - U_{eff}/kT \quad (4b)$$

The frequency dependence of the χ_M'' peak for complex **2** was determined at eight oscillation frequencies up to 1500 Hz. To supplement the ac data and thus provide for a more accurate kinetic analysis, additional relaxation *vs.* temperature data were obtained at temperatures below 1.8 K, the operating minimum of our SQUID instrument, from dc magnetization decay *vs.* time measurements. These data were obtained on single crystals using a micro-SQUID apparatus. First, a large dc field of 1.4 T was applied to the sample at about 5 K to saturate its magnetization in one direction, and the temperature was then lowered to a chosen value between 0.04 and 2.0 K. When the temperature was stable, the field was swept from 1.4 T to zero at a rate of 0.14 T s^{-1}, and then the magnetization in zero field was measured as a function of time. This gave a set of relaxation time (τ) *vs.* T data, which were combined with the ac data and used to construct an Arrhenius plot of τ *vs.* $1/T$ (Fig. 4). The data above 2.5 K ($1/T$ = 0.4 K^{-1}) were fit to the Arrhenius relationship (eqn. (4)), and the fit (dashed line in Fig. 4) gave an effective energy barrier (U_{eff}) of 67 K and a pre-exponential factor (τ_o) of 6.6×10^{-9} s. The U_{eff} value falls within the normal range 42–50 cm^{-1} (60–72 K) observed previously for several $[Mn_{12}O_{12}(O_2CR)_{16}(H_2O)_4]$ complexes.[1] Below ~2.5 K, the τ *vs.* $1/T$ plot of Fig. 4 deviates from linearity as the thermally-activated relaxation rate diminishes and the relaxation *via* quantum tunneling through the anisotropy barrier becomes more important. Eventually, at low enough temperature, the plot would plateau and become temperature-independent, as expected for the relaxation now being only *via* quantum tunneling as the thermally activated relaxation rate becomes insignificant.

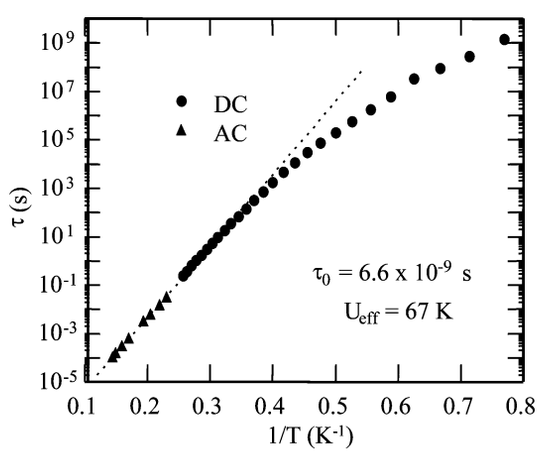

Fig. 4 Arrhenius plot for **2** using ac χ_M'' data (▲) on a microcrystalline sample and dc magnetization decay data (●) on a single-crystal. The dashed line is the fit of the data in the thermally activated region to eqn. (4); see the text for the fitting parameters.

Hysteresis studies below 1.8 K

Since complex **2** is a SMM, it should exhibit hysteresis below its blocking temperature, T_B, in a magnetization *vs.* dc field plot. Fig. 5 shows such magnetization *vs.* field scans for **2** at different temperatures in the 2.0–4.0 K range and a constant sweep rate of 4 mT s^{-1}. Hysteresis loops were indeed observed below 4.0 K, whose coercivities increase with decreasing temperature, as expected for a SMM. The loops are not completely smooth, instead showing the step-like features characteristic of quantum tunneling of the magnetization (QTM) through the anisotropy barrier. Such steps are a common feature of the hysteresis loops of many types of SMMs.[20] However, the steps in the loops for complex **2** in Fig. 5 are much less well defined than usual for $[Mn_{12}O_{12}(O_2CR)_{16}(H_2O)_4]$ complexes.[21] Instead, they are rather broad and poorly resolved, although clearly present at field positions of zero, ~0.65 and ~1.3 T. Examination of many crystals gave comparable results, the steps occasionally being almost totally smeared out. Such broadening of QTM steps is not uncommon, particularly in larger SMMs such as Mn_{18}[22a] and Mn_{30}[23b] where no sign of a step feature is evident even though the presence of QTM is confirmed from other types of data such as temperature-independent relaxation rates and quantum hole digging. The primary origins of step broadening are weak intermolecular interactions (exchange and dipolar), and a distribution of molecular environments arising from disordered solvent molecules of crystallization, partial solvent loss, ligand disorder, crystal defects, *etc.*[22,23] A distribution of molecular environments results in a distribution in D values, and thus a distribution in step positions, which depend upon the D value. As a result, the observed steps are broadened, or even smeared out if the broadening is sufficient. Since intermolecular interactions are likely to be comparable in all Mn_{12} complexes and the latter usually give well defined steps, it is likely that the main causes of step broadening in **2** are the other reasons listed above, particularly the disorder in the CH_2Cl_2 solvents of crystallization, their partial loss on removing crystals from their mother liquor, and the slight crystal damage that results from the latter.

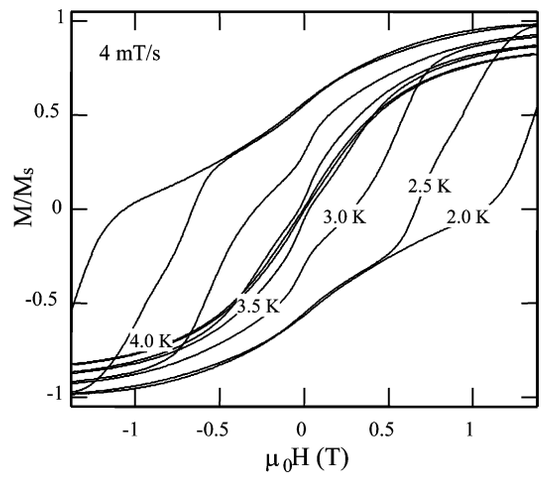

Fig. 5 Magnetization (M) *vs.* magnetic field hysteresis loops for complex **2** at the indicated temperatures and sweep rate; M is normalized to its saturation value, M_s.

Conclusions

Complete derivatization of all the axial sites with non-carboxylate ligands has been achieved for the first time in an Mn_{12} complex by replacement of the axial carboxylate ligands of **1** with $PhSO_3^-$ groups. The resultant mixed-ligand product retains both the high ground state spin value and SMM properties of the parent $[Mn_{12}O_{12}(O_2CR)_{16}(H_2O)_4]$ complexes. Complex **2** is also the first Mn_{12} species with sulfur-containing ligands and thus represents a useful expansion of this family of SMMs. In addition, with the more basic $MeCO_2^-$ groups blocking the equatorial sites, regioselective chemistry at the axial positions should now be feasible with a variety of anionic groups. Such reactions are currently under investigation.

Acknowledgements

This work was supported by the National Science Foundation. We thank the National Science Foundation and the University of Florida for funding the X-ray equipment.

References

1 G. Christou, D. Gatteschi, D. N. Hendrickson and R. Sessoli, *MRS Bulletin*, 2000, **25**, 66; R. Sessoli, H.-L. Tsai, A. R. Schake, S. Wang, J. B. Vincent, K. Folting, D. Gatteschi, G. Christou and D. N. Hendrickson, *J. Am. Chem. Soc.*, 1993, **115**, 1804; R. Sessoli, D. Gatteschi, A. Caneschi and M. A. Novak, *Nature*, 1993, **365**, 141.

2 H. J. Eppley, H.-L. Tsai, N. de Vries, K. Folting, G. Christou and D. N. Hendrickson, *J. Am. Chem. Soc.*, 1995, **117**, 301.

3 P. Artus, C. Boskovic, J. Yoo, W. E. Streib, G. Christou and D. N. Hendrickson, *Inorg. Chem.*, 2001, **40**, 4199.

4 C. Boskovic, M. Pink, J. C. Huffman, D. N. Hendrickson and G. Christou, *J. Am. Chem. Soc.*, 2001, **123**, 9914.

5 T. Lis, *Acta Crystallogr., Sect. B*, 1980, **36**, 2042.

6 G. M. Sheldrick, SHELXTL5. Bruker–AXS, Madison, WI, USA, 1998.

7 W. Wernsdorfer, *Adv. Chem. Phys.*, 2001, **118**, 99.

8 H. J. Eppley, G. Christou, N. A. Law and V. L. Pecoraro, *Inorg. Synth.*, 2002, **33**, 61.

9 C. K. Johnson and M. N. Burnett, *ORTEP–III*, Report ORNL-6895, Oak Ridge National Laboratory, TN, USA, 1996; L. J. Farrugia, *J. Appl. Crystallogr.*, 1997, **30**, 565.

10 D. Ruiz, S. M. J. Aubin, E. Rumberger, C. D. Incarvito, K. Folting, A. L. Rheingold, G. Christou and D. N. Hendrickson, *Mol. Cryst. Liq. Cryst.*, 1999, **335**, 413.

11 M. Soler, P. Artus, K. Folting, J. C. Huffman, D. N. Hendrickson and G. Christou, *Inorg. Chem.*, 2001, **40**, 4902.

12 S. M. J. Aubin, D. Ruiz, E. Rumberger, Z. Sun, B. Albela, M. W. Wemple, N. R. Dilley, J. Ribas, M. B. Maple, G. Christou and D. N. Hendrickson, *Mol. Cryst. Liq. Cryst.*, 1999, **335**, 371.

13 T. Kuroda–Sowa, S. Fukuda, S. Miyoshi, M. Maekawa, M. Munakata, H. Miyasaka and M. Yamashita, *Chem. Lett.*, 2002, **31**, 682.

14 K. Kambe, *J. Phys. Soc. Jpn.*, 1950, **5**, 48.

15 J. B. Vincent, C. Christmas, H.-R. Chang, Q. Li, P. D. W. Boyd, J. C. Huffman, D. N. Hendrickson and G. Christou, *J. Am. Chem. Soc.*, 1989, **111**, 2086; D. N. Hendrickson, G. Christou, E. A. Schmitt, E. Libby, J. S. Bashkin, S. Wang, H.-L. Tsai, J. B. Vincent, P. D. W. Boyd, J. C. Huffman, K. Folting, Q. Li and W. E. Streib, *J. Am. Chem. Soc.*, 1992, **114**, 2455.

16 J. Yoo, A. Yamaguchi, M. Nakano, J. Krzystek, W. E. Streib, L.-C. Brunel, H. Ishimoto, G. Christou and D. N. Hendrickson, *Inorg. Chem.*, 2001, **40**, 4604.

17 Z. Sun, D. Ruiz, N. R. Dilley, M. Soler, J. Ribas, K. Folting, M. B. Maple, G. Christou and D. N. Hendrickson, *Chem. Commun.*, 1999, **19**, 1973; S. M. J. Aubin, Z. Sun, H. J. Eppley, E. M. Rumberger, I. A. Guzei, K. Folting, P. K. Gantzel, A. L. Rheingold, G. Christou and D. N. Hendrickson, *Polyhedron*, 2001, **20**, 1139.

18 J. T. Brockman, K. A. Abboud, D. N. Hendrickson and G. Christou, *Polyhedron*, 2003, in press.

19 A. Abragam and B. Bleaney, *Electron Paramagnetic Resonance of Transition Ions*, Dover Press, Minneaola, NY, 1986.

20 D. N. Hendrickson, G. Christou, H. Ishimoto, J. Yoo, E. K. Brechin, A. Yamaguchi, E. M. Rumberger, S. M. J. Aubin, Z. Sun and G. Aromì, *Polyhedron*, 2001, **20**, 1479.

21 M. Soler, W. Wernsdorfer, K. A. Abboud, D. N. Hendrickson and G. Christou, *Polyhedron*, 2003, in press.

22 (*a*) E. K. Brechin, C. Boskovic, W. Wernsdorfer, J. Yoo, A. Yamaguchi, E. C. Sañudo, T. R. Concolino, A. L. Rheingold, H. Ishimoto, D. N. Hendrickson and G. Christou, *J. Am. Chem. Soc.*, 2002, **124**, 9710; (*b*) E. C. Sañudo, E. K. Brechin, C. Boskovic, W. Wernsdorfer, J. Yoo, A. Yamaguchi, T. R. Concolino, K. A. Abboud, A. L. Rheingold, H. Ishimoto, D. N. Hendrickson and G. Christou, *Polyhedron*, 2003, in press.

23 (*a*) M. Soler, E. Rumberger, K. Folting, D. N. Hendrickson and G. Christou, *Polyhedron*, 2002, **20**, 1365; (*b*) M. Soler, W. Wernsdorfer, D. N. Hendrickson and G. Christou, *J. Am. Chem. Soc.*, 2003, submitted for publication.